Glycoconj J (2014) 31:365–386
DOI 10.1007/s10719-014-9532-z

Molecular dynamics study of the conformations of glycosidic linkages in sialic acid modified ganglioside GM3 analogues

G. Jaishree · D. Jeya Sundara Sharmila

Received: 4 March 2014 / Revised: 25 April 2014 / Accepted: 21 May 2014 / Published online: 10 June 2014

Abstract The objective of the present study is to model the analogues of monosialoganglioside (GM3) by making modifications in its sialic acid residue with different substitutions in aqueous environment and to determine their structural stability based upon computational molecular dynamics. Molecular mechanics and molecular dynamics investigation was carried out to study the conformational preferences of the analogues of GM3. Dynamic simulations were carried out on the analogues of GM3 varying in the substituents at C-1, C-4, C-5, C-8 and C-9 positions of their sialic acid or Neuraminic acid (NeuAc) residue. The analogues are soaked in a periodic box of TIP3P water as solvent and subjected to a 10 ns molecular dynamics (MD) simulation using AMBER ff03 and gaff force fields with 30 ps equilibration. The analogue of GM3 with 9-*N*-succNeuAc (analogue5, C9 substitution) was observed to have the lowest energy of −6112.5 kcal/mol. Graphical analysis made on the MD trajectory reveals the direct and water mediated hydrogen bonds existing in these sialic acid analogues. The preferable conformations for glycosidic linkages of GM3 analogues found in different minimum energy regions in the conformational maps were identified. This study sheds light on the conformational preferences of GM3 analogues which may be essential for the design of GM3 analogues as inhibitors for different ganglioside specific pathogenic proteins such as bacterial toxins, influenza toxins and neuraminidases.

Keywords Ganglioside GM3 analogues · AMBER · Molecular Modeling · Molecular Mechanics · Molecular Dynamics

G. Jaishree · D. J. S. Sharmila (✉)
Department of Bioinformatics, School of Biotechnology and Health Sciences, Karunya University, Karunya Nagar, Coimbatore 641 114, Tamil Nadu, India
e-mail: djssharmila@gmail.com

Introduction

Gangliosides are group of structurally heterogeneous anionic glycosphingolipids and are characterized by the presence of one or more acidic sugar known as *N*-acetylneuraminic acid (NeuAc) or alternately as sialic acid [1]. Gangliosides exist in several types of eukaryotic cells, ubiquitously distributed on vertebrate plasma membranes [2, 3]. The structure of gangliosides comprises a long lipophilic ceramide tail and a negatively charged hydrophilic oligosaccharide portion [4]. Depending upon the number and location of sialic acid residues in their carbohydrate moiety, they are grouped as monosialo (GM), disialo (GD), trisialo (GT), and tetrasialogangliosides (GQ). They are mainly found in neural cells and in the outer-layer of plasma membranes [5] of the animal kingdom. Gangliosides can amount to 6 % of the weight of lipids from brain, where they constitute 10–12 % of the total lipid content (20–25 % of the outer layer) of neuronal membranes. GM3 is thought to be one of the key molecules of signal transduction in mammalian cells by aggregating to growth factor receptors in the membrane domains

Table 1 Ganglioside GM3 analogues with single substituent modification at C-9/C-5/C-1 positions in its NeuAc

S.NO	Ganglioside GM3 derivative	Substituents		
	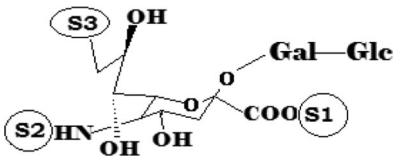	S1	S2	S3
	GM3	H	CH_3CO	HO
1.	9-Deoxy-NeuAc	H	CH_3CO	H
2.	9-Amino-NeuAc	H	CH_3CO	H_2N
3.	9-Acetamido-NeuAc	H	CH_3CO	CH_3CO-NH
4.	9-N-Gly-NeuAc	H	CH_3CO	H_2NCH_2C0-NH
5.	9-*N*-Succ-NeuAc	H	CH_3CO	$HOOC(CH_2)_2CONH$
6.	9-iodo-NeuAc	H	CH_3CO	I
7.	9-thio-NeuAc	H	CH_3CO	HS
8.	9-ScH3-NeuAc	H	CH_3CO	CH_3S
9.	5-N-fluoroac-neu	H	FCH_2CO	HO
10.	5-N-trifluoroac-Neu	H	CF_3CO	HO
11.	5-*N*-Gly-Neu	H	H_2NCH_2CO	HO
12.	5-*N*-Succ-Neu	H	$HOOC(CH_2)_2CO$	HO
13.	NeuAc-Me-ester	H_3C	CH_3CO	HO
14.	NeuAc-Et-ester	H_5C_2	CH_3CO	HO

[6]. GM3 is abundantly expressed on a number of tumours [7, 8] especially malignant melanoma. It has been reported to be potential targets for breast cancer immunotherapy [9, 10], chemotherapy [11], and radiotherapy [12]. Gangliosides bind specifically to viruses and to various bacterial toxins such as *Escherichia coli* heat-labile entero toxin [13, 14], *Helicobacter pylori* [15], *Neisseria gonorrhoeae* [16], swine rotavirus [17] and interferon [18]. Several toxins like shiga toxin/verotoxin [19] recognize GM3 and also GM3 is involved with Tay-Sachs disease [20]. Staphylococcal toxin is bound by gangliosides mainly containing *N*-acetylneuraminic acid [14]. Gangliosides serve as receptors of various toxin, they were known to be even incorporated for sensing those toxin [21]. Molecular dynamics simulation methods are applicable to study the structural and conformational aspects of biological molecules [21–25].

Present work starts with the molecular modelling of the GM3 analogues with the substituted NeuAc having single and multiple substituents at C-1, C-4, C-5, C-8 and C-9 positions. Molecular mechanics and molecular dynamics calculations are performed to have a vivid picture about the conformational preference of monosialoganglioside GM3 analogues in aqueous solution. The direct and water mediated hydrogen bonds which play a major role in the structural stability of GM3 are also analyzed.

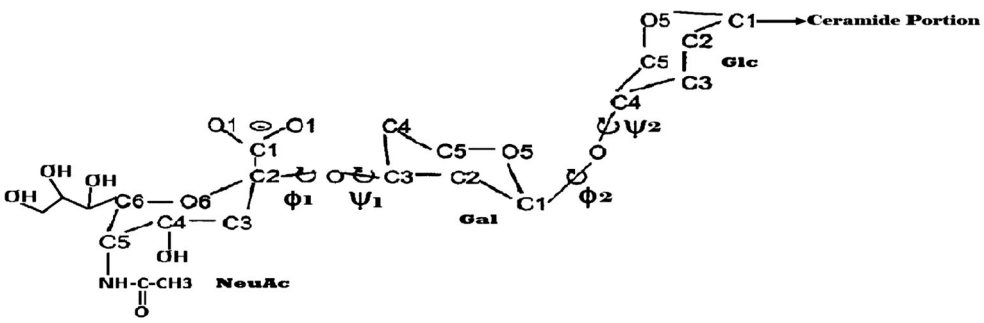

Fig. 1 Numbering of Atoms and dihedral angle of Monosialoganglioside, GM3 Abbreviations: NeuAc, *N*-Acetyl Neuraminic Acid; Gal, Galactose; Glc, Glucose

Table 2 Ganglioside GM3 analogues with multiple modifications at with C-1/C-4/C-8/C-9 positions in its NeuAc

S.NO	Ganglioside GM3 derivative	Substituents			
		M1	M2	M3	M4
	GM3	H	H	OH	OH
1.	Methyl 5-*N*-acetyl Neuraminate	CH_3	H	OH	OH
2.	Benzyl 2-α-*O*-methyl-5-*N*-acetyl-8,9-O-isopropylidene Neuraminate	CH_2Ph	H	OCH_3	OCH_3
3.	Benzyl 2-α-*O*-methyl-4-*O*-Capriloyl-5-*N*-α-acetyl-8,9-*O*-isopropylidene Neuraminate	CH_2Ph	$CO_2(CH_2)_6CH_3$	OCH_3	OCH_3
4.	Benzyl 2-α-*O*-methyl-4-*O*-Capriloyl-5-*N*-α-acetyl- Neuraminate	CH_2Ph	$CO_2(CH_2)_6CH_3$	OH	OCH_3
5.	2α-*O*-methyl-4-*O*-Capriloyl-5-*N*-α-acetyl- Neuraminic acid	H	$CO_2(CH_2)_6CH_3$	OH	OCH_3
6.	Benzyl 2-α-*O*-methyl-4-*O*-(8-morpholin)-Capriloyl-5-*N*-α-acetyl-8,9-*O* Isopropylidene Neuraminate	CH_2Ph	$CO_2(CH_2)_7O(CH_2CH_2)_2NH$	OCH_3	OCH_3
7.	Benzyl 2-α-*O*-methyl-4-*O*-(8-morpholin) Capriloyl-5-*N*-acetyl-Neuraminate	CH_2Ph	$CO_2(CH_2)_7O(CH_2CH_2)_2NH$	OH	OH
8.	2-α-*O*-methyl-4-*O*-(8-morpholin)-Capriloyl-5-*N*-α-acetyl-Neuraminic acid	H	$CO_2(CH_2)_7O(CH_2CH_2)_2NH$	OH	OH
9.	5-*N*-Acetyl-9-amino -9-deoxy-Neuraminic acid	H	H	OH	NH_2

Materials and methods

Molecular dynamics and molecular mechanics of GM3 analogues varying in the neuraminic acid substituents at positions C-9/C-5/C-1: structural and conformational implications

GM3 analogues with single substituents modeled in this study are compiled in Table 1 [26]. The synthetic GM3 analogues are modelled as described by Oetke *et al*., (2002) [27]. The numbering of atoms and dihedral angles involved in generating different conformational structures for GM3 ganglioside are taken from earlier studies [28] and shown in Fig. 1.

The initial conformations of the different dihedral angles of GM3 analogues are as follows:

If NeuAc is involved in the linkage, the initial conformation was defined as

$\Phi_1 = 0$ when C1−C2 cis to O−C3 and

$\psi_1 = 0$ when C2−O cis to C3−H3.

Table 3 Minimum energy conformations of GM3 analogues with single substituents at C-9/C-5/C-1 Position in its NeuAc in aqueous environment

S.NO	Derivative	Relativeenergy (kcal/mol)	(Φ_1,Ψ_1) Degrees	(Φ_2,Ψ_2) Degrees
	GM3	0	(−51.07, 54.09)	(81.34, 58.57)
1.	9-DeoxyNeuAc	−9.2	(46.76, 4.73)	(65.37, 53.39)
2.	9-AminoNeuAc	−25.2	(−49.49, 63.80)	(76.03, 60.53)
3.	9-AcetamidoNeuAc	−35.4	(−29.32, 43.48)	(69.16, 51.37)
4.	9-*N*-GlyNeuAc	27.5	(61.12, −27.05)	(95.95, 61.81)
5.	9-N-SuccNeuAc	−121.3	(46.84, 0.69)	(75.24, 55.75)
6.	9-iodo-NeuAc	4.6	(−48.15, 70.24)	(65.12, 47.96)
7.	9-thio-NeuAc	−20.5	(−49.98, 58.78)	(53.77, 42.93)
8.	9-ScH3-NeuAc	−44.8	(43.40, 9.47)	(80.68, 60.00)
9.	5-*N*-fluoroac-Neu	−0.8	(−12.71, 50.72)	(82.11, 62.55)
10.	5-*N*-Trifluoroac-Neu	75.7	(−41.32, 41.29)	(57.97, 44.69)
11.	5-*N*-Gly-Neu	51.1	(−4.6, 50.22)	(50.79, 41.36)
12.	5-*N*-succ-Neu	−46.5	(140.89, 35.13)	(148.76, 39.21)
13.	NeuAc-Me-ester	17.9	(−45.71, 55.72)	(65.93, 55.67)
14.	NeuAc-Et-ester	39.6	(−41.37, 54.75)	(55.10, 47.19)

The glycosidic conformation for the non-NeuAc involved disaccharide fragments of the monosialoganglioside GM3 analogues were defined as

$\Phi_2 = 0$ when H1−C1 cis to O−CX
$\psi_2 = 0$ when C1−*O* cis to CX−HX

(Where X represents the number of Carbon atom involved in the glycosidic linkage).

Molecular Mechanics calculations were carried out in the Pentium IV workstation using SANDER module of AMBER 10 [29] software. The force fields AMBER ff03 and gaff (general amber force fields) that incorporate the Cornell *et al.*, (1995) [30] force fields were used. Water molecules were added from the solvent library of AMBER10 and care is taken to maintain the number of water molecules same for all the GM3 derivatives.

A periodic box enclosing the analogues in solution was constructed to turn into a periodic system for the simulation program and periodic boundary conditions are applied on constant volume. The non-bonded cut off was specified at 8 Å. For initial 100 cycles steepest descent method was used, then conjugate gradient is switched on. The convergence criterion for the energy gradient is less than 0.01 kcal mole-1. The energy minimized structures for all the GM3 derivatives are intensively analyzed through VEGA ZZ to find out the direct and solvent mediated hydrogen bonds.

To understand the conformational dynamics of GM3 analogues in aqueous environment, molecular dynamics calculations were performed over a period of 30 ps equilibrium followed by a 10 ns production run with explicit inclusion of water molecules. The width of integration step of the MD simulation was 1 fs. The history of information was recorded for every 1000 steps of trajectory which resulted in 10,000 structures. The temperature was maintained to be 300 k. The total simulation time was around 25 h 25 min for each molecule. The MD trajectory information collected for every 1 ps was analyzed using PTRAJ (Trajectory Analysis) module for AMBER 10 package.

Molecular dynamics of neuraminic acid with multiple substituents at position C-1/C-4/C-8/C-9 in the GM3 analogues: structural and conformational implications

The modeled GM3 derivatives with C-1/C-4/C-8/C-9 NeuAc substituted analogues are shown in Table 2 [26]. The GM3 derivatives are designed as described by Sauter *et al.*, (1992) [31] and Bianco *et al.*, (1998) [32]. The initial conformations of the different dihedral angles of GM3 analogues are defined as mentioned earlier and subjected to Molecular mechanics and molecular dynamics calculations.

Fig. 2 Projection of global minimum energy conformer of GM3 analogues varying in the NeuAc Substituents **a** 9-deoxy-NeuAc, **b** 9-AminoNeuAc, **c** 9-AcetamidoNeuAc, **d** 9-*N*-GlyNeuAc, **e** 9-*N*-SuccNeuAc, **f** 9-iodo-NeuAc, **g** 9-thio-NeuAc, **h** 9-ScH3-NeuAc, **i** 5-*N*-fluoroac-Neu, **j** 5-*N*-Trifluoroac-Neu, **k** 5-*N*-Gly-Neu, **l** 5-N-succ-Neu, **m** NeuAc-Me-ester, **n** NeuAc-Et-ester in aqueous environment

Results and discussion

Molecular dynamics and molecular mechanics of GM3 analogues varying in the NeuAc substituents at position C-9/C-5/C-1: structural and conformational implications

Relative energy of GM3 analogues

The minimum energy conformers of GM3 analogues with their relative molecular mechanics energy profile are tabulated in Table 3. The relative energy is calculated for all the 14 GM3 analogues with respect to the absolute minimum energy of GM3 (−5991.2 Kcal/mol). The GM3 analogues with 9-*N*-succNeuAc (analogue5, C9 substitution) and 9-ScH3-NeuAc (analogue 8, C9 substitution) are observed to have minimum energy such as −121.3 kcal/mol and −44.8 kcal/mol respectively. The GM3 analogues with 5-*N*-Succ-Neu (analogue 12, C5 substitution) and 9-AcetamidoNeuAc (analogue3, C9 Substitution) are found to have minimum energy such as −46.5 kcal/mol and −35.4 kcal/mol, respectively. The GM3 analogues with 9-AminoNeuAc (analogue 2, C9 substitution) and 9-thio-NeuAc (analogue 7, C9 substitution) showed minimum energy such as −25.2 kcal/mol and −20.5 kcal/mol respectively. The GM3 analogues 9-DeoxyNeuAc (analogue 1, C9 substitution) and 5-*N*-fluoroac-Neu (analogue 9, C5 substitution) are calculated to have minimum energy such as −9.2 kcal/mol and −0.8 kcal/mol respectively. It is apparent from Table 3 that, in the minimum energy conformation for the analogues of GM3 with 9-*N*-succNeuAc and 9-ScH3-NeuAc, the glycosidic angle for α-NeuAc-(2–3)-β-Gal linkage (Φ_1, Ψ_1) prefer to be around (46.84, 0.69) and (43.40, 9.47) respectively. The minimum energy conformation for the analogues of GM3 with 5-N-Succ-Neu and 9-AcetamidoNeuAc, the glycosidic angle for α-NeuAc-(2–3)-β-Gal linkage (Φ_1, Ψ_1) prefer to be around (140.89, 35.13) and (−29.32, 43.48), respectively. The minimum energy conformation for the analogues of GM3 with 9-AminoNeuAc and 9-thio-NeuAc, the

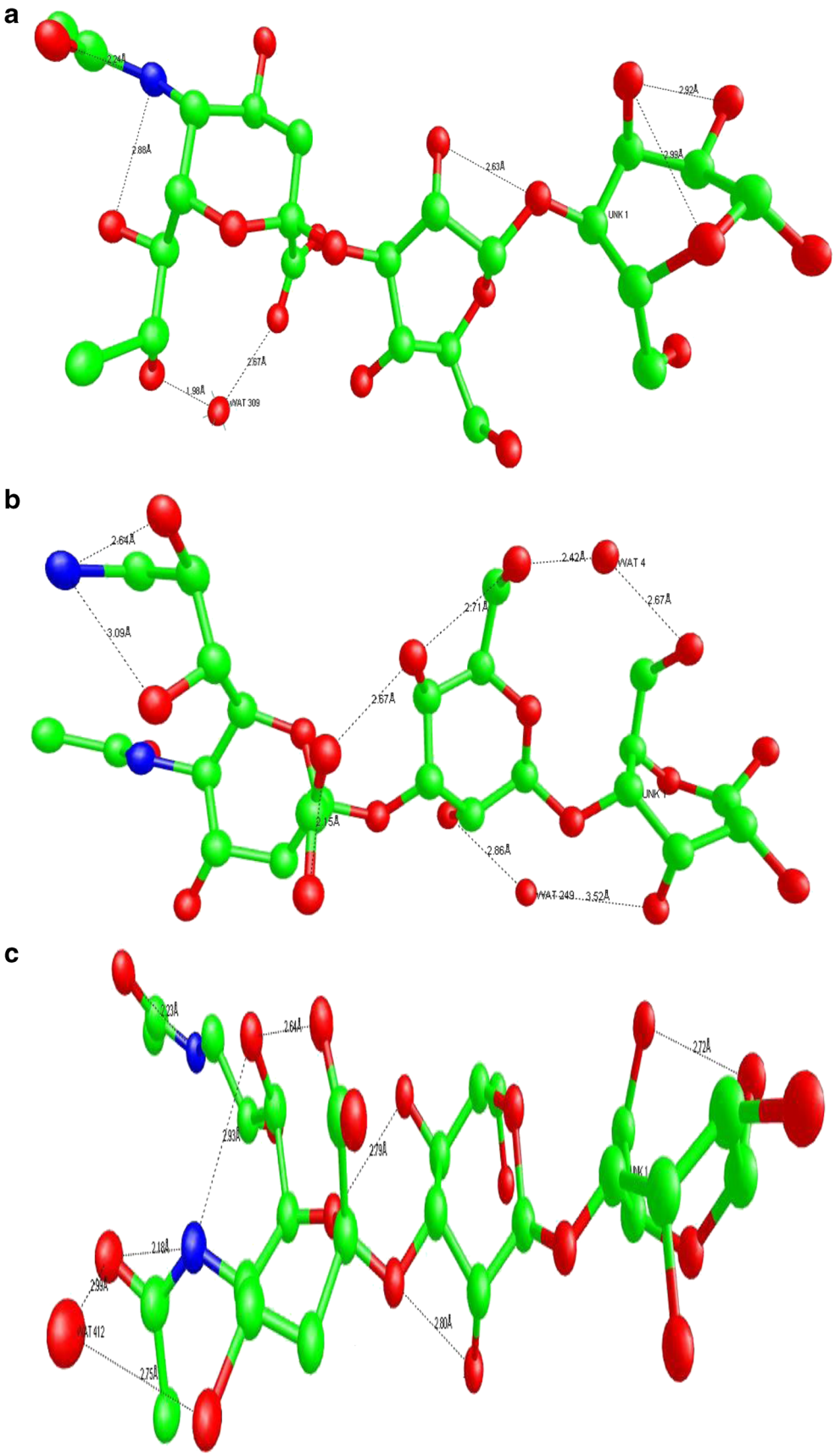
a
2.74Å
2.88Å
2.63Å
2.92Å
2.99Å
UNK 1
2.67Å
1.98Å
WAT 309
b
2.64Å
3.09Å
2.42Å
WAT 4
2.71Å
2.67Å
2.67Å
2.15Å
2.86Å
WAT 249
3.52Å
c
2.23Å
2.64Å
2.72Å
2.93Å
2.79Å
2.18Å
2.99Å
WAT 412
2.75Å
2.80Å

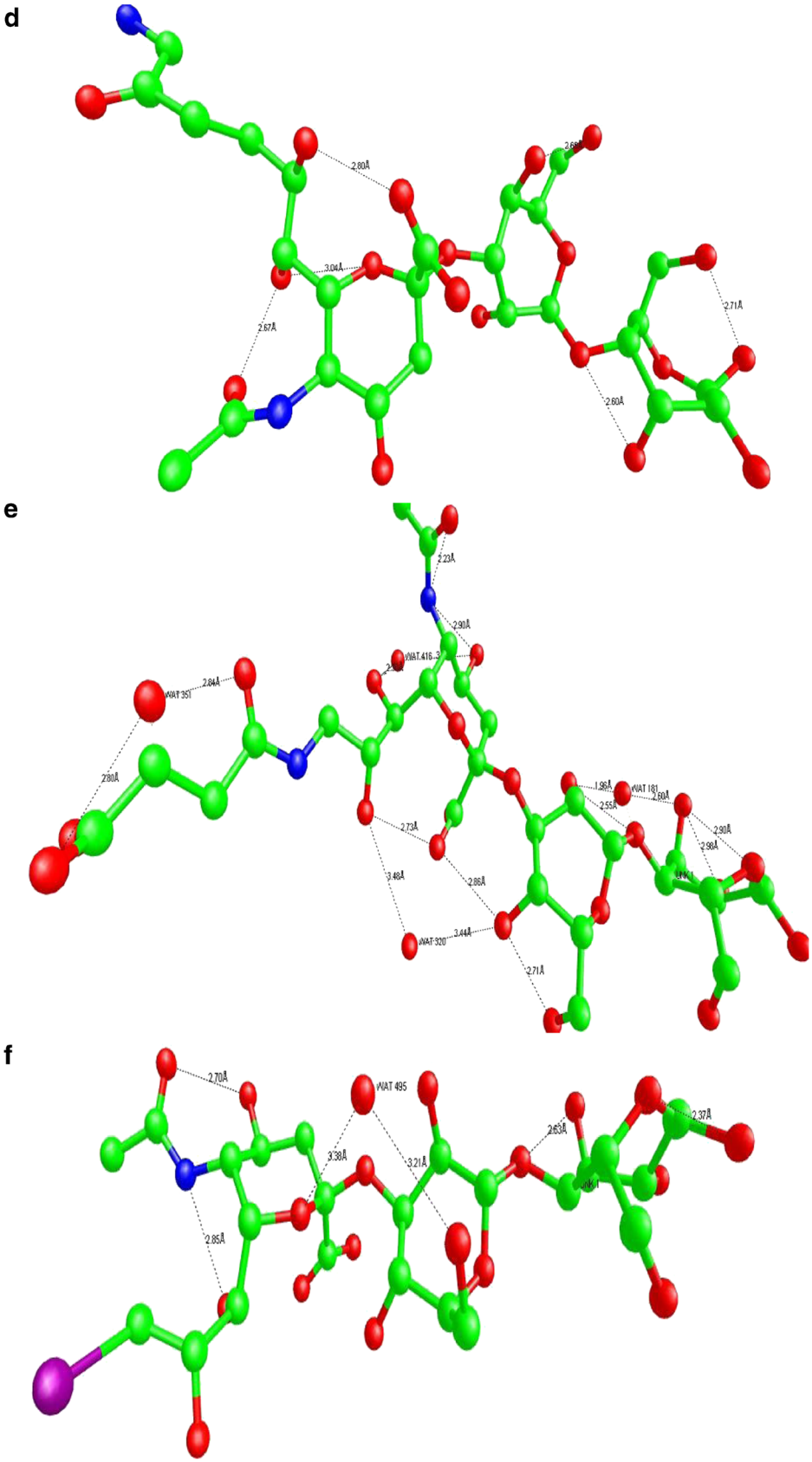

Fig. 2 (continued)

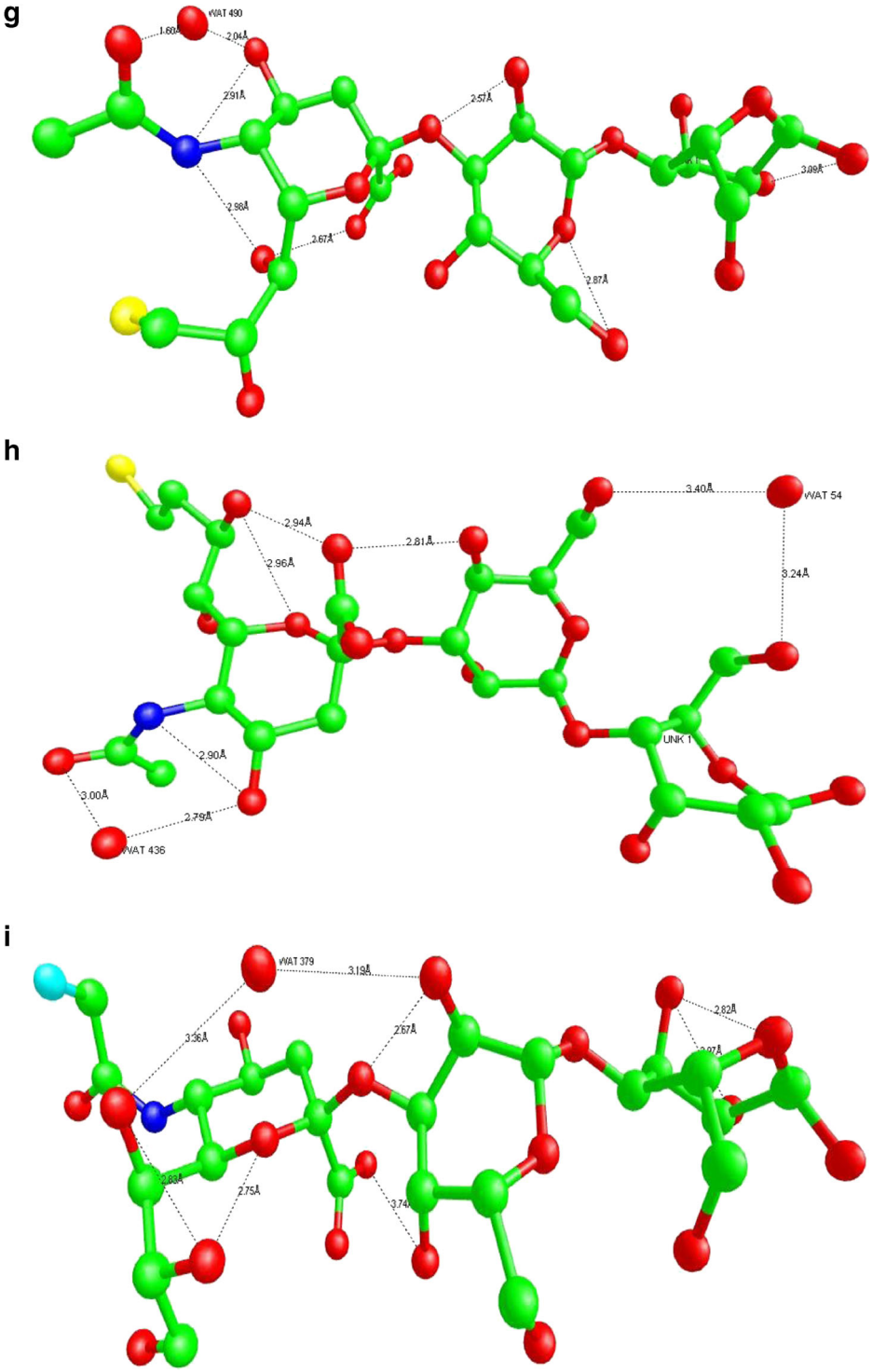

Fig. 2 (continued)

glycosidic angle for α-NeuAc-(2–3)-β-Gal linkage (Φ_1, Ψ_1) prefer to be around (−49.49, 63.80) and (−49.98, 58.78), respectively. The minimum energy conformation for the analogues of GM3 with 9-DeoxyNeuAc and 5-*N*-fluoroac-Neu, the glycosidic angle for α-NeuAc-(2–3)-β-Gal linkage (Φ_1, Ψ_1) prefers to be around (46.76, 4.73) and (12.71, 50.72) respectively. The glycosidic angle (Φ_2,Ψ_2) for β-Gal-(1–4)-β-Glc linkage of the

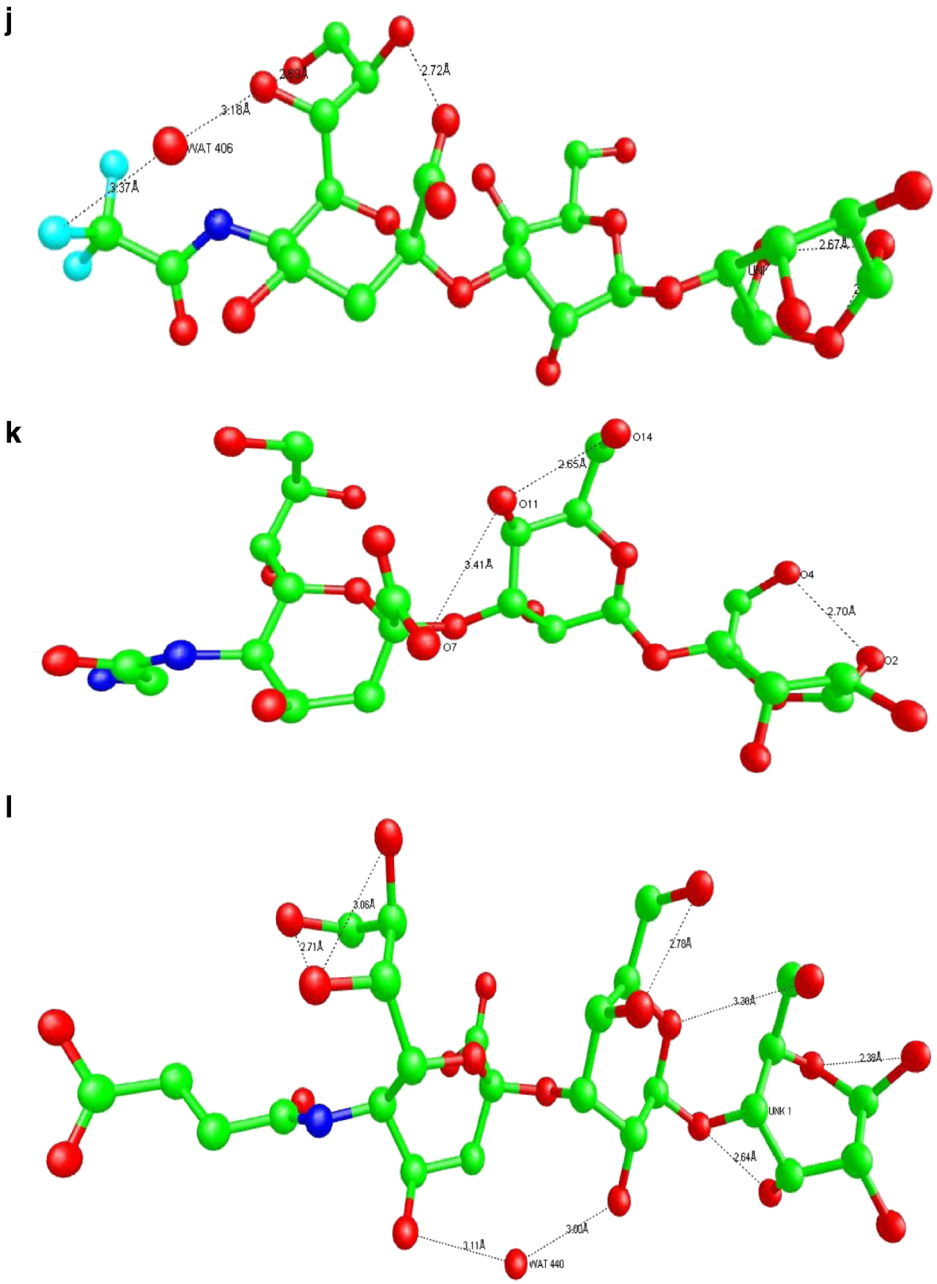

Fig. 2 (continued)

above said all eight molecules prefers to be around (75.24, 55.75), (80.68, 60.00), (148.76, 39.21), (69.16, 51.37), (76.03, 60.53), (3.77, 42.93), (65.37, 53.39) and (82.11, 62.55), respectively. It is evident from previous research by Sharmila and Veluraja, 2004 that the glycosidic linkage between galactose and glucose prefers to be rigid, which is also proved in the present study. The torsional angles (Φ_1, Ψ_1) revealed for α-NeuAc-(2–3)-β-Gal linkage in the present GM3 analogues is also supported by the NMR studies reported [33, 34] for other similar gangliosides.

Role of hydrogen bonds in structural stability

Graphical analysis of the global minimum energy conformer of GM3 analogues in aqueous environment manifests that water plays a crucial role in stabilizing this conformational state by the formation of bridging

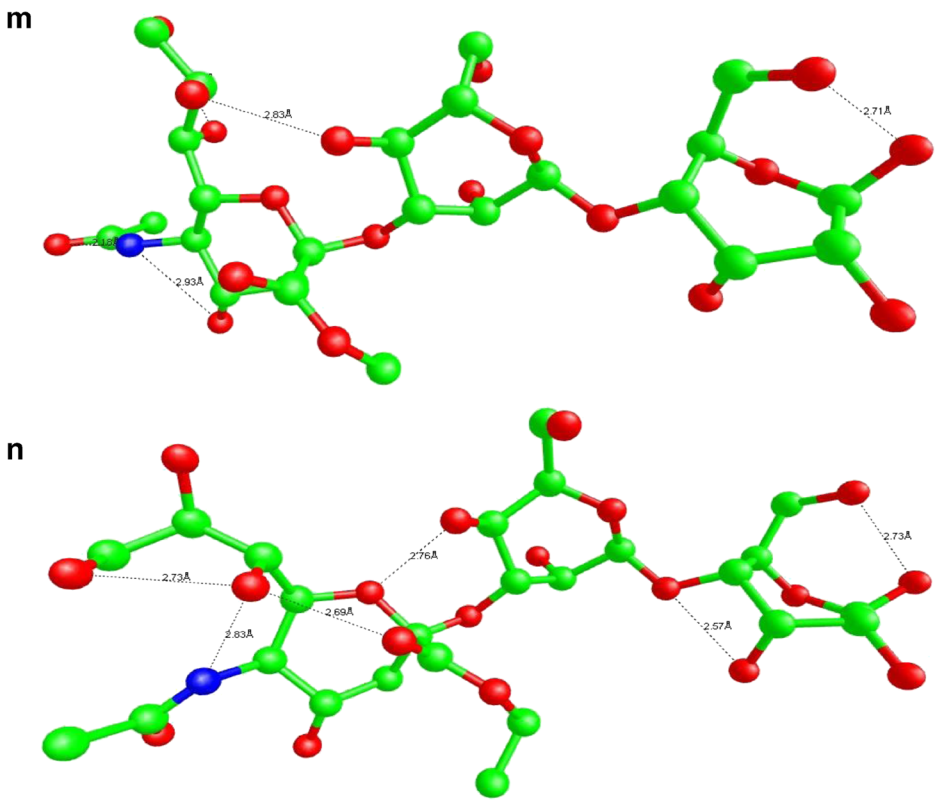

Fig. 2 (continued)

hydrogen bonds between different atoms. The three dimensional structure of GM3 analogues in global minimum energy conformation state, which shows the water mediated hydrogen bonds and direct hydrogen bonds are displayed in Fig. 2a–n. The force of attraction, shown in the Fig. 2 a–n as a dotted line, is the hydrogen bond. Table 4 represents the hydrogen bonds predicted for each GM3 analogue with interacting sialic acid atoms and distances. Water mediated hydrogen bonds play a dominant role in stabilizing the conformational structures of GM3 derivatives.

A comparison of the total number of direct together with the water mediated hydrogen bonds in the minimum energy conformers of GM3 analogues with modified NeuAc revealed that 9-*N*-Succ-Neu has four water mediated hydrogen bonds and eight direct hydrogen bonds. A total of one water mediated Bonds and six direct hydrogen bonds has been observed for the energy minimized structure of GM3 analogue with 9-Acetamido-NeuAc. Energy minimized structure of GM3 analogue with 9-ScH3-NeuAc has two water mediating hydrogen bonds and four direct hydrogen bonds. GM3 analogue with ethyl group substituted at C1 position of 5-*N*-succ-Neu is recorded with a single water mediating hydrogen bond and six direct hydrogen bonds. The energy differences between the GM3 analogues can be well accounted for the differences in hydrogen bonding. So it is well understood that hydrogen bonds correspond to their stability.

Molecular dynamics of GM3 analogues

To study the conformational dynamics of GM3 derivatives, molecular mechanics calculations were performed and a 10 ns molecular dynamics simulation was carried out. An in-depth analysis on the conformational features of all the 14 GM3 analogues (C9, C5, C1 Substituted NeuAc) were carried out over the frames collected for every 1 ps in the trajectory.

C-9 substituted side chain conformation

Figure 3a–c describes the molecular dynamic trajectory showing transitions of torsion angles (Φ_1,Ψ_1) of GM3 analogues 2, 5 and 8 solvated with water. Figure 4a–c describes the molecular dynamic trajectory showing transitions of torsion angles (Φ_2,Ψ_2) of GM3 analogues 2, 5 and 8 solvated with water. In GM3 analogue with

Table 4 Hydrogen Bond in each GM3 analogue with single substituent modification at C-9/C-5/C-1 positions in its NeuAc

S.NO	GM3 Derivative	Interacting GM3 derivative atom 1	Mediating water	Distance (Å)	Interacting GM3 derivative atom 2	Distance (Å)
1.	9-DeoxyNeuAc	O6	WAT 309	2.56	O16	2.40
		O12			O10	2.63
		O3			O	2.99
		O3			O1	2.92
		N			O17	2.88
		N			O15	2.24
2.	9-AminoNeuAc	O14	WAT 04	2.42	O4	2.67
		O10	WAT 249	2.86	O3	3.52
		O16			N	2.64
		O11			O6	2.67
		N			O17	3.09
		O11			O14	2.71
		O7			O6	2.15
3.	9-Acetamido NeuAc	O16	WAT 412	1.87	N	3.01
		O15			N	2.18
		N			O17	2.93
		O17			O6	2.64
		O5			O11	2.79
		O18			N1	2.23
		O4			O2	2.72
4.	9-*N*-GlyNeuAc	O16			O6	2.80
		O16			O5	3.15
		O15			O17	2.67
		O12			O3	2.60
		O11			O14	2.68
5.	9-*N*-Succ NeuAc	O8	WAT 416	3.44	O17	2.30
		O11	WAT 320	3.44	O16	3.48
		O3	WAT 181	2.60	O10	2.96
		O19	WAT 351	2.80	O18	2.84
		O3			O	2.90
		O12			O10	2.55
		O6			O16	2.73
		O14			O11	2.71
		O3			O1	2.98
		O6			O11	2.86
		N			O15	2.23
		N			O8	2.90
6.	9-iodo-NeuAc	O5	WAT 495	3.38	O11	3.21
		N			O17	2.85
		O6			O17	3.00
		O15			O8	2.70
		O13			O3	2.37
7.	9-thio-NeuAc	O15	WAT 490	1.60	O8	2.04
		O17			N	2.98
		O17			O6	2.67
		O13			O10	2.57
		O9			O14	2.87
		O1			O10	3.09
		N			O8	2.91

Table 4 (continued)

S.NO	GM3 Derivative	Interacting GM3 derivative atom 1	Mediating water	Distance (Å)	Interacting GM3 derivative atom 2	Distance (Å)
8.	9-ScH3-NeuAc	O14	WAT 54	3.40	O4	3.24
		O15	WAT 436	3.00	O8	2.79
		O16			O6	2.94
		O16			O5	2.96
		O6			O11	2.81
		N			O8	2.90
9.	5-*N*-fluoroac-Neu	O10	WAT 379	3.36	O18	3.19
		O			O3	2.82
		O3			O1	2.97
		O7			O11	3.74
		O13			O10	2.67
		O5			O17	2.75
		O18			O17	2.83
10.	5-*N*-Trifluoroac-Neu	O18	WAT 406	3.18	F1*	3.37
		O6			O17	2.72
		O18			N	2.78
		O16			O18	2.69
		O			O2	2.38
		O2			04	2.67
11.	5-*N*-Gly-Neu	O2			O4	
		O7			O11	2.70
		O11			O14	3.41
						2.65
12.	5-*N*-succ-Neu	O8	WAT 440	3.11	O10	3.00
		O18			O16	2.71
		O18			O17	3.06
		O12			O3	2.64
		O14			O11	2.78
		O			O2	2.38
		O9			O4	3.30
13.	NeuAc-Me-ester	O15			N	2.18
		O17			O11	2.83
		O16			O18	2.82
		O13			O10	2.64
		O12			O3	2.55
14.	NeuAc-Et-ester	O18			O16	2.73
		O18			N	2.83
		O6			O18	2.69
		O5			O11	2.76
		O12			O3	2.57
		O2			O4	2.73

* is the atom from the substituent group

9-AminoNeuAc (analogue 2), the (Φ_1, Ψ_1) graph shows distribution between (−60, 60) and (−120, 0). In Ramachandran Map, it shows as two clusters A and B. A region is present at (−49.49, 63.80) and B region at (−120, 0). The A region is much preferred than B and its conformation is shown in Fig. 2b. In GM3 analogue with 9-*N*-Succ-NeuAc (analogue 5), there is a clear shift in (Φ_1, Ψ_1) from (46.84, 0.69) to (−120, 30)

regions. It is clearly seen in Ramachandran Map with 2 distinct domains A: (120, 30) and B: (46.84, 0.69), However, A region is much preferred. This confirmation of A region is shown in the Fig. 5 and B region in Fig. 2e.

In GM3 analogue with 5-ScH3-NeuAc (analogue 8), the (Φ_1, Ψ_1) plot remains to be prominent in (43.40, 9.47) (*i.e.*) B region. The ramachandran plot shows 2 clusters A and B, where B region is prominent; which is present at (43.40, 9.47) region, its conformation is shown in Fig. 2h. It is found from literature review [35, 36] that the glycosidic linkage between Gal-β-(1–4)-β-Glc is bit rigid and it prefers to be in (60, 60), and it is also observed as the same in the present results as shown in the following Figs. 4a–c, 6b and 7a, b.

C-5 and C-1 substituted side chain conformation

Figure 6a, b represents the dynamic behavior of torsions (Φ_1, Ψ_1) and (Φ_2, Ψ_2) along with distribution plot of GM3 analogue with 5-N-Succ-Neu (analogue 12) in aqueous environment. In GM3 analogue with 5-N-Succ-Neu, (Φ_1, Ψ_1) graph, the plot remains steady in (140.89, 35.13) region and the ramachandran plot also shows a single domain (A) at (140.89, 35.13), which implies that the succinamide group in glycerol side chain (R3) does not affect the linkage (as normal in GM3). But in amido side chain substitution, it affects the linkage by not allowing to be normal (−60) global minimum value. The present study reports the application of Molecular dynamics and Molecular mechanics simulation techniques in the determination of the three-dimensional structures of synthetic GM3 analogues varying in the different NeuAc substituent positions of C-9/C-5/C-1. This study is helpful to understand their conformational preference and structural stability to interact with their natural receptors. The focus of the present study is on the preferable conformations as well as the minimum energy or predominant conformation of the molecule. The preferable conformation of GM3

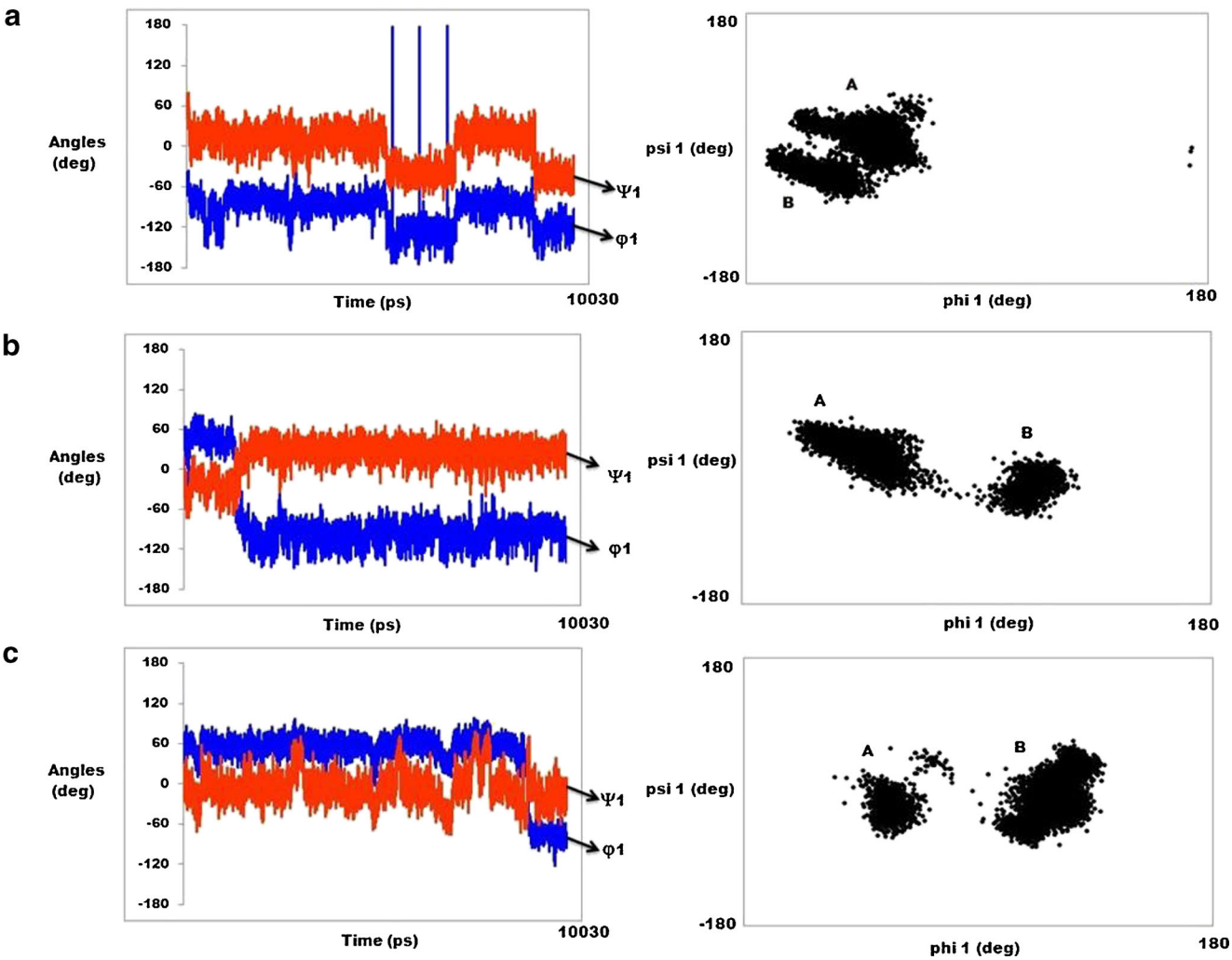

Fig. 3 Molecular Dynamics trajectory and distribution plots of (Φ_1, Ψ_1) **a** 9-AminoNeuAc **b** 9-N-Succ-NeuAc **c** 5-ScH3-NeuAc in GM3 analogues

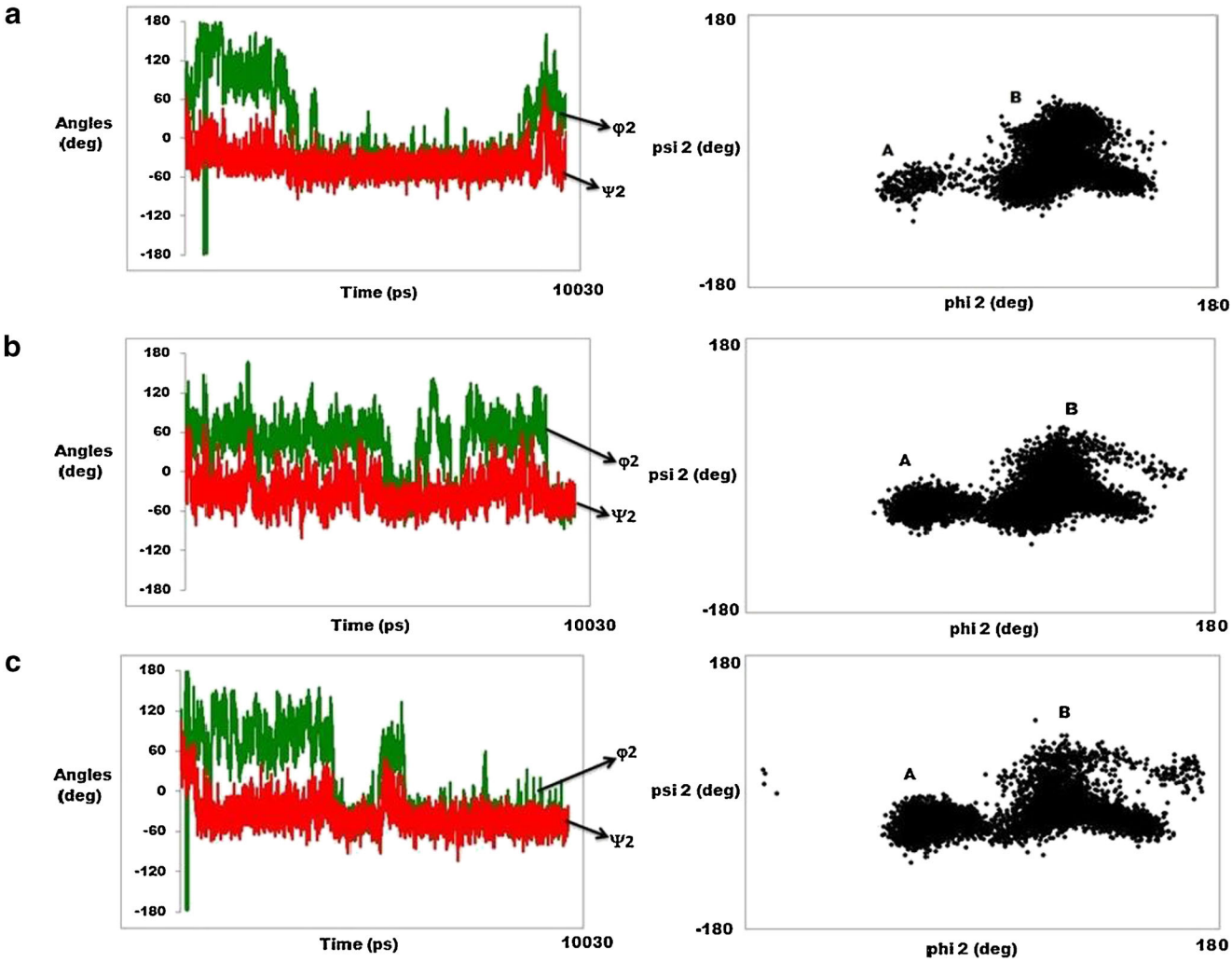

Fig. 4 Molecular Dynamics trajectory and distribution plots of (Φ_2, Ψ_2) **a** 9-AminoNeuAc **b** 9-N-Succ-NeuAc **c** 5-ScH3-NeuAc in GM3 analogues

analogues varying in different dihedral angle linkages was observed by the present molecular dynamics study correlates well with those reported for similar linkages in various α-NeuAc-(2–3)-β-Gal and Gal-β-(1–4)-β-Glc

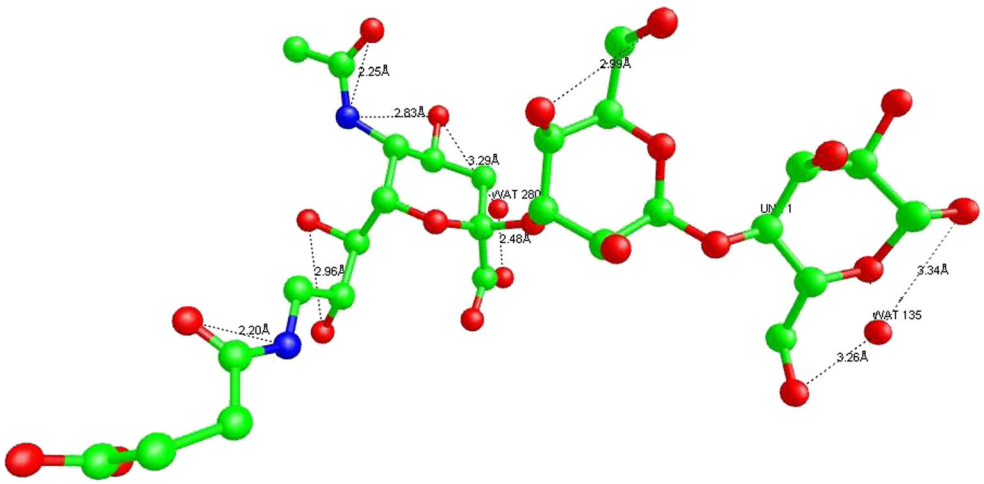

Fig. 5 New conformation of GM3 analogue with 9-*N*-Succ-NeuAc

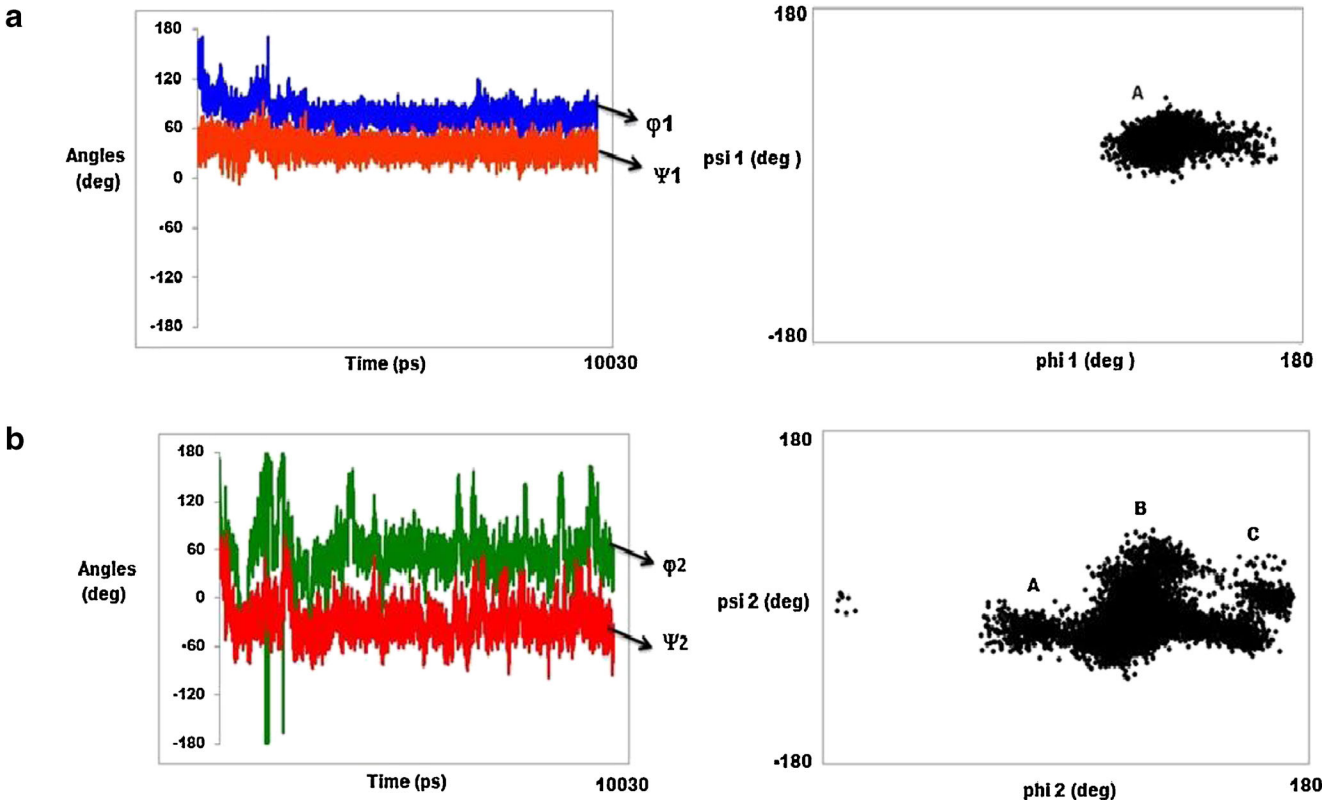

Fig. 6 Molecular Dynamics trajectory and distribution plots **a** (Φ_1, Ψ_1) **b** (Φ_2, Ψ_2) of 5-N-Succ-Neu in GM3 analogues

moieties present in all the di- and tri- sialogangliosides by earlier studies [35].

Molecular dynamics of GM3 analogues with multiple substituents at position C-1/C-4/C-8/C-9: structural and conformational implications

Relative energy of GM3 derivatives

The relative energy is calculated for all the 9 GM3 derivatives with respect to the absolute minimum energy of GM3 (−5991.2 kcal/mol). The minimum energy conformation of GM3 derivatives with respect to their relative energy are displayed in Table 5. The GM3 analogue with modified NeuAc such as, Analogue 9 (5-*N*-Acetyl-9-amino −9-deoxy-Neuraminic acid), analogue5 (2α-*O*-methyl-4-*O*-Capriloyl-5-*N*-acetyl-Neuraminic acid), analogue 1 (methyl 5-N-acetyl Neuraminate) are found to have the minimum energy −20.3 kcal/mol, −44.9 kcal/mol and −0.4 kcal/mol respectively. The minimum energy dihedral angle (Φ_1,Ψ_1) for α-NeuAc-(2–3)-β-Gal linkage for analogue9 (5-*N*-Acetyl-9-amino −9-deoxy-Neuraminic acid), analogue5 (2α-*O*-methyl-4-*O*-Capriloyl-5-*N*-acetyl-Neuraminic acid), analogue 1 (methyl 5-*N*-acetyl Neuraminate) prefer to be around (53.08, 61.90), (66.74, 131.92) and (−40.23, 35.47), respectively. And the glycosidic angle (Φ_2,Ψ_2) for Gal-β-(1–4)-β-Glc linkage prefer values around (75.56, 58.99), (59.22, 53.33) and (74.70, 47.91), respectively.

Contribution of hydrogen bonds in structural stability

Figure 7 and Table 6 show the formation of water mediated hydrogen bonds and direct hydrogen bonds in GM3 derivatives. It is well known from previous findings that water mediated hydrogen bonds formed within the molecule plays a major role in stabilization of the molecule [37] especially of gangliosides [38].

Fig. 7 Projection of global minimum energy conformer of GM3 analogues varying in the NeuAc Substituents **a** methyl 5-*N*-acetyl Neuraminate, **b** Benzyl 2α-*O*-methyl-5-n-acetyl-8,9-*O*-isopropylidene Neuraminate, **c** Benzyl 2α-*O*-methyl-4-*O*-Capriloyl-5-*N*-acetyl-8,9-*O*-isopropylidene Neuraminate, **d** Benzyl 2α-*O*-methyl-4-O-Capriloyl-5-*N*-acetyl-Neuraminate, **e** 2α-*O*-methyl-4-O-Capriloyl-5-*N*-acetyl-Neuraminic acid, **f** 2-α-*O*-methyl-4-*O*-(8-morpholin)-Capriloyl-5-*N*-acetyl-Neuraminic acid, **g** 5-*N*-Acetyl-9-amino −9-deoxy-Neuraminic acid in aqueous environment

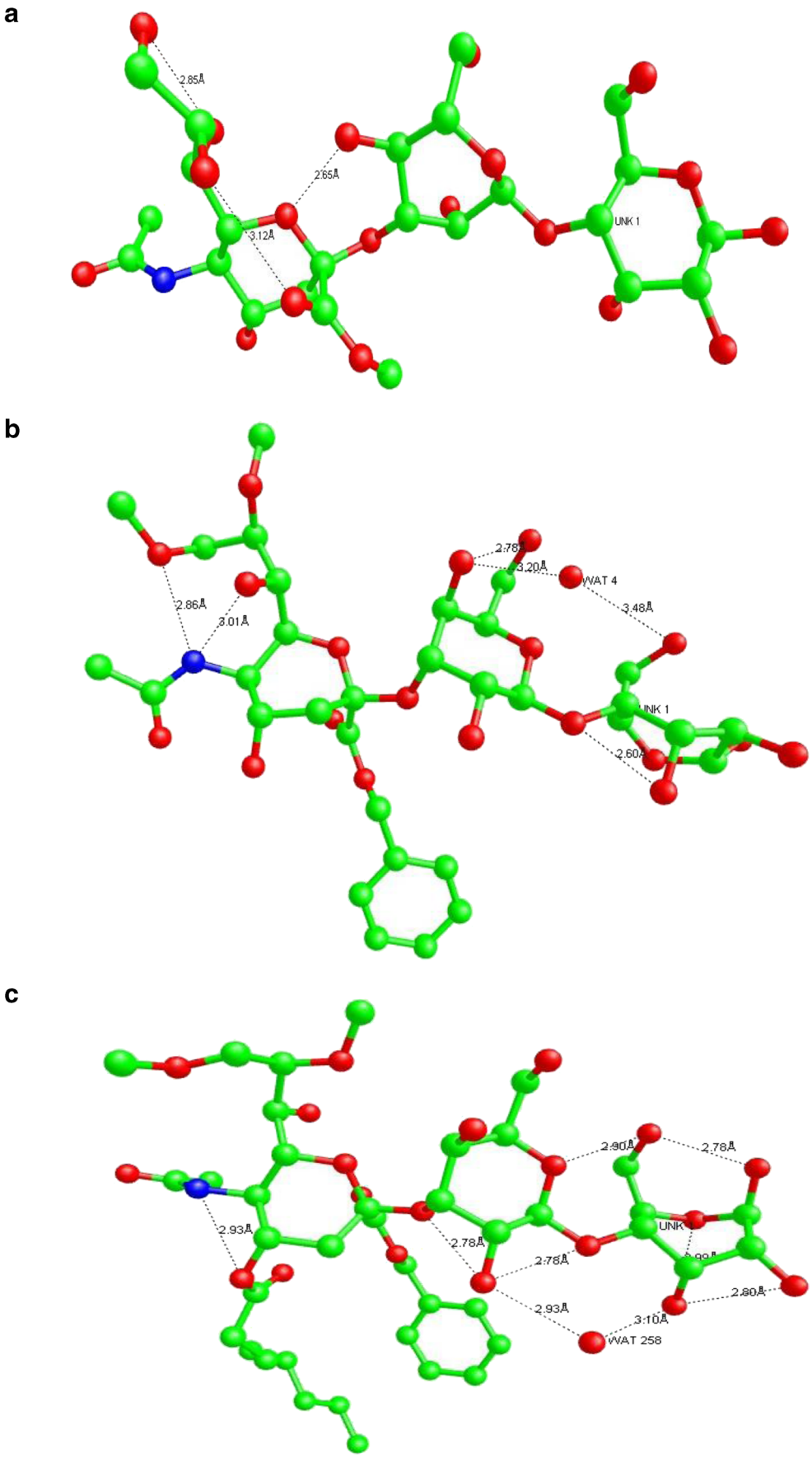
a
2.85Å
2.65Å
3.12Å
UNK 1
b
2.78Å
3.20Å
WAT 4
3.48Å
2.86Å
3.01Å
UNK 1
2.60Å
c
2.90Å
2.78Å
2.93Å
UNK 1
2.78Å
2.78Å
2.80Å
2.93Å
3.10Å
WAT 258

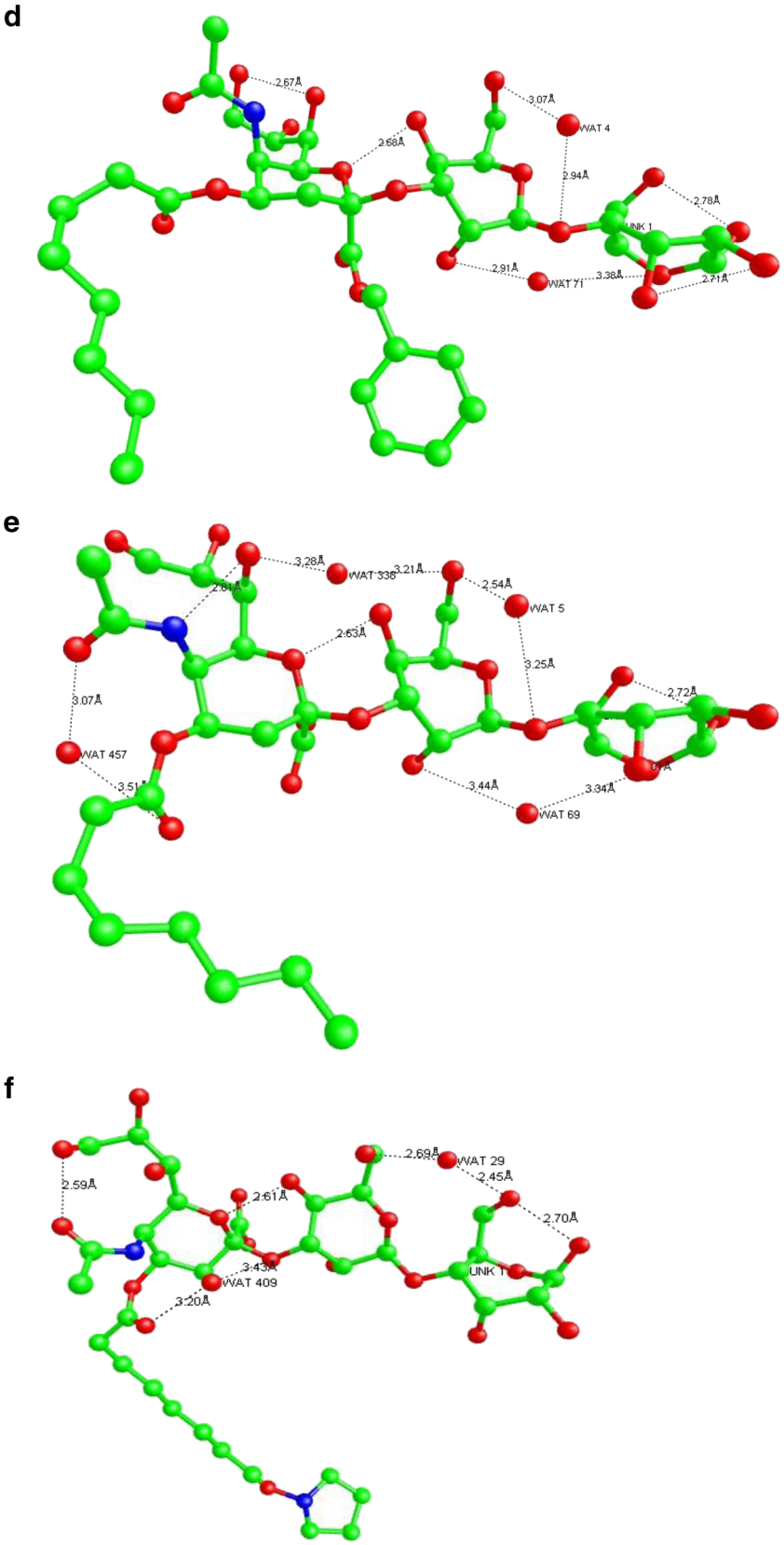

Fig. 7 (continued)

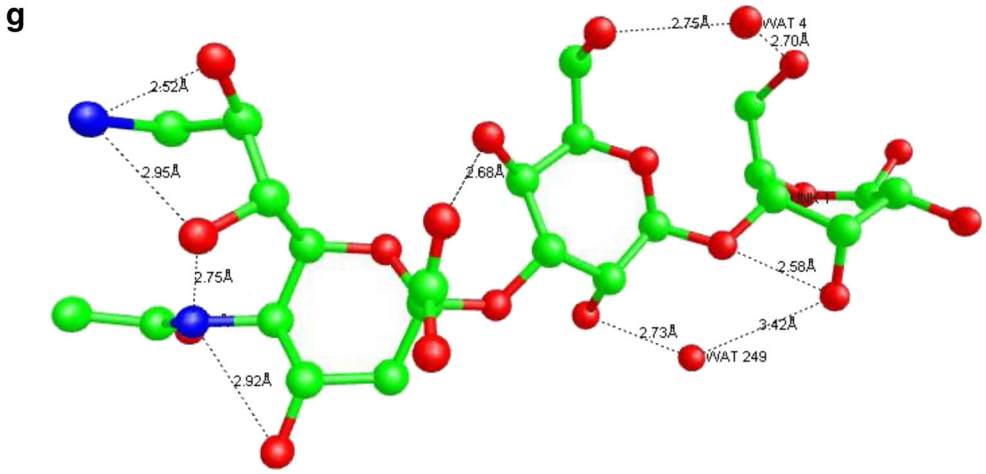

Fig. 7 (continued)

Comparison of water mediated hydrogen bonds with direct hydrogen bonds revealed that GM3 analogues having their NeuAc modified shows that, analogue 1 (methyl 5-N-acetyl Neuraminate) has three direct hydrogen bonds. Analogue 2 (Benzyl 2α-O-methyl-5-n-acetyl-8,9-O-isopropylidene Neuraminate) has one water mediating hydrogen bond and four direct hydrogen bonds. Analogue 3 (Benzyl 2α-O-methyl-4-O-Capriloyl-5-N-n-acetyl-8,9-O-isopropylidene Neuraminate) shows one water mediating hydrogen bonds and seven direct hydrogen bonds. Analogue 4 (Benzyl 2alpha-O-methyl-4-O-Capriloyl-5-N-n-acetyl- Neuraminate) has two water mediating hydrogen bonds and four direct hydrogen bonds. Analogue 5 (2α-O-methyl-4-O-Capriloyl-5-N-n-acetyl-Neuraminic acid) has four water mediating hydrogen Bonds and four direct hydrogen bonds. Analogue 8 (2α-O-methyl-4-O-(8-morpholin)-Capriloyl-5-N-n-acetyl-Neuraminic acid) shows two water mediating hydrogen bonds and three direct hydrogen bonds. Analogue 9 (5-N-Acetyl-9-amino −9-deoxy-Neuraminic acid) has two water mediating hydrogen Bonds and seven direct hydrogen bonds. It is inferred that the maximum number of direct and water mediated hydrogen bonds present in each GM3 derivatives are responsible for the minimum energy and its stabilization of the molecule.

Molecular dynamics of GM3 analogues

To study the conformational dynamics of all the neuraminic acid derivatives, a 10 ns molecular

Table 5 Minimum Energy conformation of GM3 analogues with multiple substituents at C-1/C-4/C-8/C-9 Position in its NeuAc

S.NO	Derivative GM3	Relative energy (kcal/mol) 0	(Φ_1, Ψ_1) degrees (−51.07, 54.09)	(Φ_2,Ψ_2) degrees (81.34, 58.57)
1.	Methyl 5-*N*-acetyl Neuraminate	−0.4	(−40.23, 35.47)	(74.70, 47.91)
2.	Benzyl 2α-*O*-methyl-5-*N*-acetyl-8,9-*O*-isopropylidene Neuraminate	29.8	(171.29, 33.53)	(102.06, 54.3)
3.	Benzyl 2α-O-methyl-4-*O*-Capriloyl-5-*N*-acetyl-8,9-*O*-isopropylidene Neuraminate	22.2	(175.76, 33.77)	(94.87, 55.03)
4.	Benzyl 2α-*O*-methyl-4-*O*-Capriloyl-5-*N*-acetyl- Neuraminate	41.4	(67.64, 156.17)	(64.64, 65.86)
5.	2α-*O*-methyl-4-*O*-Capriloyl-5-*N*-acetyl- Neuraminic acid	−44.9	(66.74, 131.92)	(59.22, 53.33)
6.	Benzyl 2α-*O*-methyl-4-*O*-(8-morpholin)-Capriloyl-5-*N*-acetyl-8, 9-O-Isopropylidene Neuraminate	26.1	(122.24, 56.67)	(36.17, 22.17)
7.	Benzyl 2α-*O*-methyl-4-*O*-(8-morpholin)-Capriloyl-5-*N*-acetyl-Neuraminate	27.3	(−40.44, 26.50)	(78.21, 64.36)
8.	2α-*O*-methyl-4-*O*-(8-morpholin)-Capriloyl-5-*N*-acetyl-Neuraminic acid	31.4	(75.29, 101.31)	(66.94, 61.54)
9.	5-*N*-Acetyl-9-amino −9-deoxy-Neuraminic acid	−20.3	(−53.08, 61.90)	(75.56, 58.99)

Table 6 Hydrogen Bond in each GM3 analogue with multiple modifications at C-1/C-4/C-8/C-9 Position in its NeuAc

S.NO	GM3 derivative	Interacting GM3 derivative atom 1	Mediating water	Distance (Å)	Interacting GM3 derivative atom 2	distance (Å)
1.	Methyl 5-*N*-acetyl Neuraminate	O16			O18	2.85
		O17			O6	3.12
		O5			O11	2.65
2.	Benzyl 2-α-O-methyl-5-*N*-acetyl-8, 9-O-isopropylidene Neuraminate	O11	WAT 4	3.20	O4	3.48
		O16*			N	2.86
		O18*			N	3.01
		O11			O14	2.78
		O12			O3	2.60
3.	Benzyl 2-α-*O*-methyl-4-*O*-Capriloyl-5-*N*-acetyl-8,9-*O*-isopropylidene Neuraminate	O10	WAT 258	2.93	O3	3.10
		O10			O12	2.78
		O10			O13	2.78
		O3			O1	2.80
		O9			O4	2.90
		O4			O2	2.78
		O3			O	2.99
		O8			N	2.93
4.	Benzyl 2-α-*O*-methyl-4-*O*-Capriloyl-5-*N*-acetyl- Neuraminate	O10	WAT 71	2.91	O	3.38
		O14	WAT 4	3.07	O12	2.94
		O5			O11	2.68
		O1			O3	2.71
		O16*			O18	2.67
		O2			O4	2.78
5.	2-α-*O*-methyl-4-*O*-Capriloyl-5-*N*-acetyl-Neuraminic acid	O15	WAT 457	3.07	O19*	3.51
		O10	WAT 69	3.44	O	3.34
		O18	WAT 338	3.28	O14	3.21
		O14	WAT 5	2.54	O12	3.25
		O18			N	2.81
		O5			O11	2.63
		O2			O4	2.72
		O			O3	3.01
6.	Benzyl 2-α-*O*-methyl-4-*O*-(8-morpholin)-Capriloyl-5-N-acetyl-8,9-*O*-Isopropylidene Neuraminate	O16			O18	2.65
		O12			O10	2.76
		O2			O4	2.71
		O8			N	2.93
7.	Benzyl 2-α-*O*-methyl-4-*O*-(8-morpholin)-Capriloyl-5-*N*-acetyl-Neuraminate	O4			O14	2.86
8.	2-α-*O*-methyl-4-*O*-(8-morpholin)-Capriloyl-5-*N*-acetyl-Neuraminic acid	O14	WAT 29	2.69	O4	2.45
		O19*	WAT 409	3.20	O13	3.43
		O15			O16	2.59
		O5			O11	2.61
		O4			O2	2.70
9.	5-*N*-Acetyl-9-amino −9-deoxy-Neuraminic acid	O4	WAT 4	2.70	O4	2.75
		O10	WAT 249	2.73	O3	3.42
		O16			N*	2.52
		O17			N*	2.95
		O17			N	2.75
		O6			O11	2.68
		O12			O3	2.58
		O8			N	2.92
		O15			N	2.24

* is the atom from substituent group

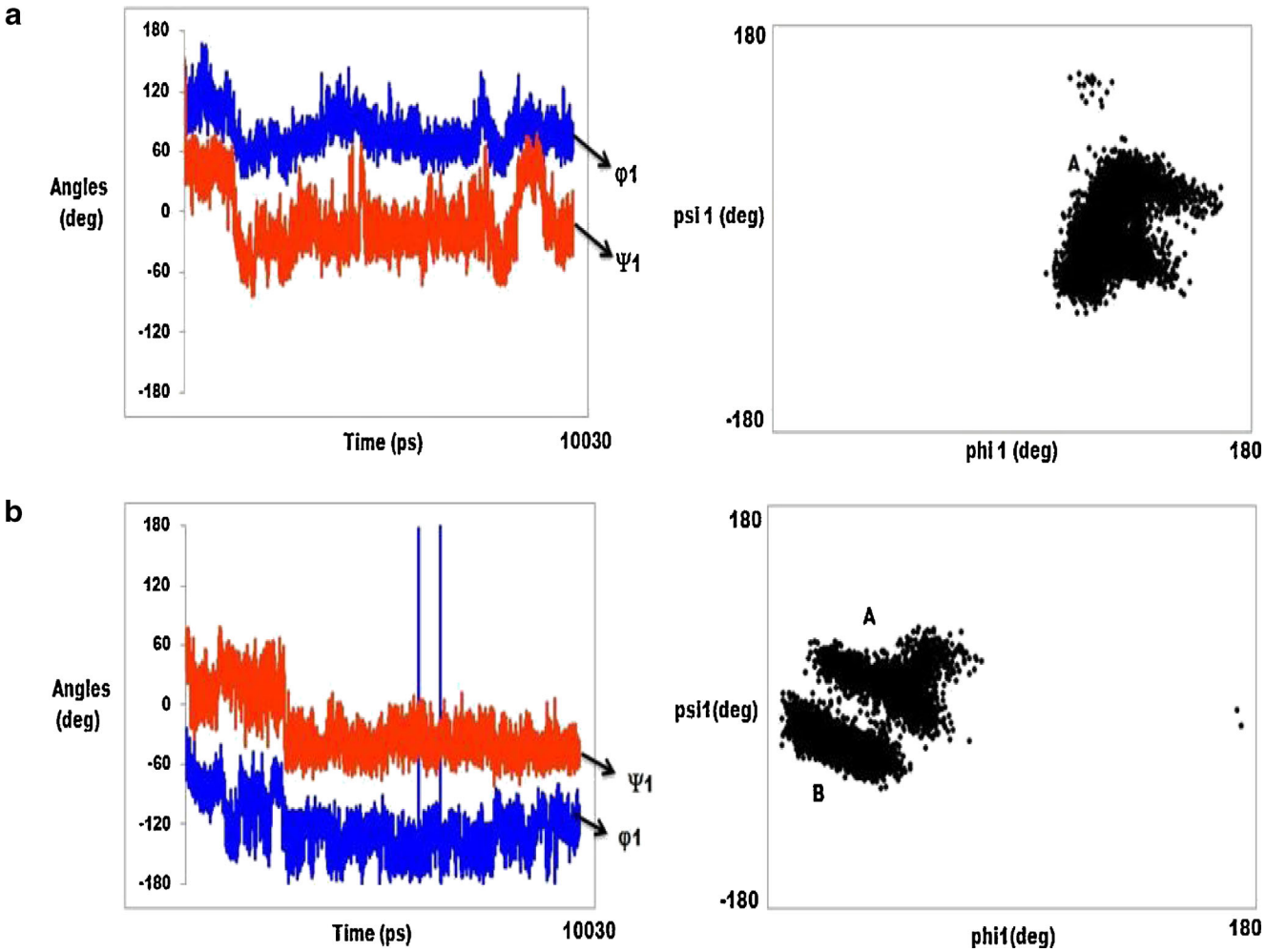

Fig. 8 **a**, **b** Molecular Dynamics trajectory and distribution plots of Φ_1, Ψ_1 **a** Benzyl 2α-O-methyl-4-O-(8-morpholin)-Capriloyl-5-N-n-acetyl-8,9-O-Isopropylidene Neuraminate **b** 5-N-Acetyl-9-amino −9-deoxy-Neuraminic acid in GM3 analogues

dynamics simulation was carried out. An in-depth analysis on the conformational features of all the 9 GM3 analogues was done by collecting the frames for every 1 ps.

C-1/C-4/C-8/C-9 substituted NeuAc in GM3 analogues

Figure 8a, b describes the molecular dynamic trajectory showing transitions of (Φ_1,Ψ_1) along with distribution plot of GM3 analogue 6 having (Benzyl2α-*O*-methyl-4-*O*-(8-morpholin)-Capriloyl-5-*N*-acetyl-8,9-*O*-Isopropylidene Neuraminate) solvated with water. Figure 9a, b describes the molecular dynamic trajectory showing transitions of (Φ_2,Ψ_2) along with distribution plot of GM3 analogue 9 possessing (5-*N*-Acetyl-9-amino −9-deoxy-Neuraminic acid) solvated with water. In GM3 analogue with Benzyl-2α-*O*-methyl-4-*O*-(8-morpholin)-Capriloyl-5-*N*-acetyl-8,9-*O*-Isopropylidene Neuraminate, the ($\Phi_1\Psi_1$) graph indicates that, on the onset, the ($\Phi_1\Psi_1$) remains around (90°, 120°) region. The ramachandran map also shows a clustered region at (66.74°, 131.92°). In GM3 analogue with 5-*N*-Acetyl-9-amino-9-deoxy-Neuraminic acid, ($\Phi_1\Psi_1$) plot starts at (−60, 60) and ends at (−120,-30). The Ramachandran map shows 2 domains (A and B), in which A is present at (−60, 60) and B is present around (−120, −30) region.

Summary and conclusion

The present study provides accessible conformational models of Ganglioside GM3 analogues with single substituent or with multiple substituents at positions C-1/C-5/C-8/C-9 in aqueous environment. Direct and

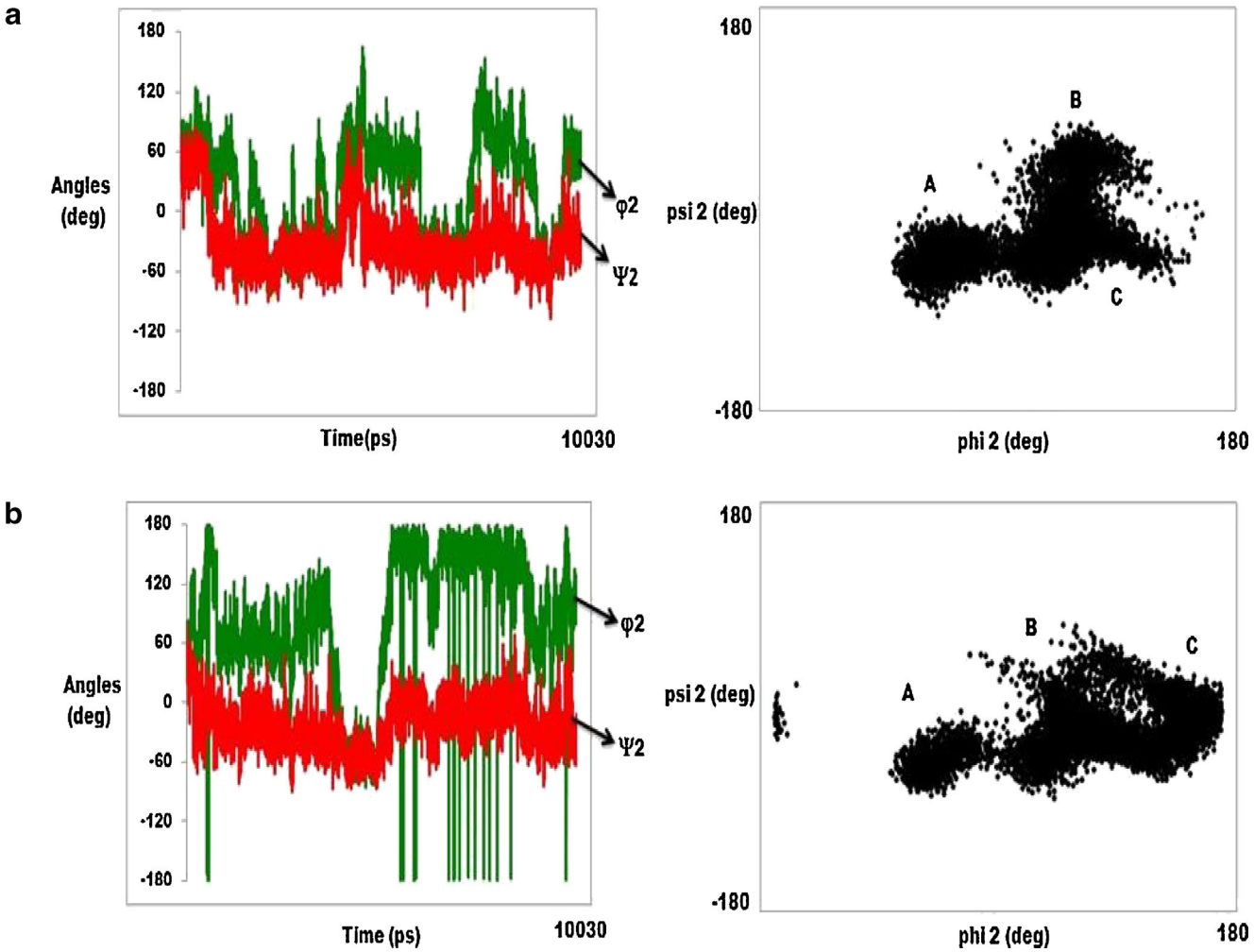

Fig. 9 **a**, **b** Molecular Dynamics trajectory and distribution plots of Φ_2,Ψ_2 **a** Benzyl 2α-O-methyl-4-O-(8-morpholin)-Capriloyl-5-N-n-acetyl-8,9-O-Isopropylidene Neuraminate **b** 5-N-Acetyl-9-amino −9-deoxy-Neuraminic acid in GM3 analogues

water mediated hydrogen bonding interaction play a dominant role in stabilizing the conformational structures in these GM3 analogues. This study also reveals dynamics trajectory and steric map for the substituent holding side chain linkages of GM3 analogues. The analogue of GM3 with 9-*N*-succNeuAc (analogue5, C9 substitution) is observed to have the lowest energy of −6112.5 kcal/mol when compared to other GM3 analogues with single and multiple substituents. Also it shows good results in hydrogen bonding interactions with four water mediated hydrogen bonds and eight direct hydrogen bonds. The NeuAc binding sites of various GM3 binding proteins are very important for the mechanism of action of the proteins. If one wants to inhibit the action of GM3 binding pathogenic proteins towards cell membrane, one should block the NeuAc binding site by designing a suitable drug based on rational designing. The GM3 analogues present in this study may be crucial for the design of GM3 analogues as inhibitors for different GM3 specific pathologic proteins such as viral/bacterial toxins and neuraminidases.

Acknowledgments The authors acknowledge the Science and Engineering Research Board (SERB), Department of Science and Technology, Govt. of India (SERB Sanction no. SR/FT/LS-157/2009 dt 30.04.2012) - OYS scheme project grant sanctioned to the corresponding author.

References

1. Bacia, K., Scherfeld, D., Kahya, N., Schwille, P.: Fluorescence correlation spectroscopy relates rafts in model and native membranes. Biophys. J. **87**, 1034–1043 (2004)
2. Huwiler, A., Kolter, T., Pfeilschifter, J., Sandhoff, K.: Physiology and pathophysiology of sphingolipid metabolism and signaling. Biochim. Biophys. Acta **1485**, 63–99 (2000)
3. Leeden, R.W., Yu, R.K.: Gangliosides: Structure, isolation and analysis. Methods Enzymol. **83**, 139–191 (1982)
4. Ishida, H., Kiso, M.: Chemical synthesis of bioactive oligosaccharides. systematic syntheses of gangliosides. Trends Glycosci. Glycotech. **13**, 57–64 (2001)
5. McDaniel, R.V., McIntosh, T.J.: X-Ray diffraction studies of the cholera toxin receptor, GM1. BioPhy. J. **49**, 94–96 (1986)
6. Hashiramoto, A., Mizukami, H., Yamashita, T.: Ganglioside GM3 promotes cell migration by regulating MAPKand c-Fos/AP-1. Oncogene **25**, 3948–3955 (2006)
7. Dyatlovitskaya, E.V., Kandyba, A.G.: Sphingolipids in tumor metastases and angiogenesis. Biochem. Mosc. **71**, 347–353 (2006). PMID: 16615853
8. Bada, A.M., Casac, A., Mancebo, A., Fuentes, D., Gonz¡lez, B.: Acute and repeated dose intramuscular toxicity of GM3 cancer vaccine in SD rats. Pak. J. Biol. Sci. **8**, 1045–1050 (2005)
9. Carr, A., Rodriguez, E., Mdel, C.A., Camacho, R., Osorio, M., et al.: Immunotherapy of advanced breast cancer with a heterophilic ganglioside (NeuGcGM3) cancer vaccine. J. Clin. Oncol. **21**, 1015–1021 (2003)
10. Guthmann, M.D., Castro, M.A., Zinat, G., Venier, C., Koliren, L., et al.: Cellular and humoral immune response to N-Glycolyl-GM3 elicited by prolonged immunotherapy with an anti-idiotypic vaccine in high-risk and metastatic breast cancer patients. J. Immunother. **29**, 215–223 (2006)
11. Basu, S., Ma, R., Boyle, P.J., Mikulla, B., Bradley, M., et al.: Apoptosis of human carcinoma cells in the presence of potential anti-cancer drugs: III. Treatment of Colo-205 and SKBR3 cells with: Cis -platin, tamoxifen, melphalan, betulinic acid, L-PDMP, L-PPMP, and GD3 ganglioside. Glycoconj. J. **20**, 563–577 (2004)
12. Oliva, J.P., Valdes, Z., Casaco, A., Pimentel, G., Gonzalez, J., et al.: Clinical evidences of GM3 (NeuGc) ganglioside expression in human breast cancer using the 14 F7 monoclonal antibody labelled with (99 m)Tc. Breast Cancer Res. Treat. **96**, 115–121 (2006)
13. Nawar, H.F., Arce, S., Russell, M.W., Connell, T.D.: Mucosal adjuvant properties of mutant lt-iia and lt-iib enterotoxins that exhibit altered ganglioside-binding activities. Infect. Immun. **73**, 1330–1342 (2005)
14. Nawar, H.F., Berenson, C.S., Hajishengallis, G., Takematsu, H., Mandell, L., Clare, R.L., Connell, T.D.: Binding to gangliosides containing N-acetylneuraminic acid is sufficient to mediate the immunomodulatory properties of the nontoxic mucosal adjuvant LT-IIb(T13I). Clin. Vaccine Immunol. **17**, 969–978 (2010). PMID: 20392887
15. Lingwood, C.A.: Glycolipid receptors for verotoxin and *helicobacter pylori*: role in pathology. Biochim. Biophys. Acta **1455**, 375–386 (1999)
16. Hugosson, S., Angstrom, J., Olsson, B.M., Bergstrom, J., Fredlund, H., Olcen, P.: Glycosphingolipid binding specificities of *Neisseria meningitides* and *Haemophilus influenza*: Detection, isolation and characterization of a binding-active glycosphingolipid from human oropharyngeal epithelium. J. Biochem. **124**, 1138–1152 (1998)
17. Rolsma, M.D., Kuhlenschmidt, T.B., Gelberg, H.B., Kuhlenschidt, M.S.: Structure and function of a ganglioside receptor for porcine rotavirus. J. Virol. **72**, 9079–9091 (1998)
18. Vengris, V.E., Reynolds Jr., F.H., Hollenberg, M.D., Pitha, P.M.: Interferon action: role of membrane gangliosides. Virology **72**, 486–493 (1976)
19. Lingwood, C.A.: Shiga toxin receptor glycolipid binding. Pathol. Utility, Methods Mol. Med **73**, 165–186 (2003)
20. Li, Y., Li, S., Hasegawa, A., Ishida, H., Kiso, M., et al.: Structural basis for the resistance of tay-sachs ganglioside GM2 to enzymatic degradation. J. Biol. Chem. **274**, 10014–10018 (1999)
21. Singh, A.K., Harrison, S.H., Schoeniger, J.S.: Gangliosides as receptors for biological toxins: development of sensitive fluoroimmunoassays using ganglioside-bearing liposomes. Analyt. Chem. **72**, 6019–6024 (2000)
22. Bagchi, A., Ghosh, T.C.: Structural and functional characterization of SoxW-a thioredoxin involved in the transport of reductants during sulfur oxidation by the global sulfur oxidation reaction cycle. Res. J. Microbiol. **1**, 392–400 (2006)
23. Bagchi, A., Ghosh, T.C.: Homology modeling and molecular dynamics study of the interactions of SoxY and SoxZ: the central player of biochemical oxidation of sulfur anions in pseudaminobacter salicylatoxidans. Res. J. Microbiol. **2**, 569–576 (2007)
24. Bouarkat, M., Sabeur, S.A., Bouamrane, R.: Investigating the formation of helical states in the process of homopolymer collapse using molecular dynamics simulations. J Applied Sciences **10**, 209–214 (2010)
25. Maftouni, N., Amininasab, M., Kowsari, F.: Molecular dynamics study of nanobio membranes. J Applied Sciences **11**, 1062–1065 (2011)
26. Sharmila, D.J.S., Jaishree, G., Rapheal, V.S.: Ganglioside GM3 analogues as inhibitors for staphylococcal enterotoxin B and endoglycoceramidase II from *Rhodococcus Sp*. – docking and ADME screening studies. Asian J. Pharma. Hea. Sci **2**, 359–369 (2012)
27. Oetke, C., Brossmer, R., Mantey, L.R., Hinderlich, S., Isecke, R., et al.: Versatile biosynthetic engineering of sialic acid in living cells using synthetic sialic acid analogues. J. Biol. Chem. **277**, 6688–6695 (2002)
28. Sharmila, D.J.S., Veluraja, K.: Monosialogangliosides and their interaction with cholera toxin-investigation by molecular modelling and molecular mechanics. J. Biomol. Struct. Dyn. **21**, 591–614 (2004)
29. Case, D.A., Darden, T.A., Cheatham, T.E., Simmerling, C.L., Wang, J., et al.: Amber 10: Users' manual. University of California, San Francisco (2008)
30. Cornell, W.D., Cieplak, P., Bayly, C.I., Gould, I.R., Merz, K.M., et al.: A second generation force field for the simulation of proteins, nucleic acids and organic molecules. J. Am. Chem. Soc. **117**(19), 5179–5197 (1995)
31. Sauter, N.K., Hanson, J.E., Glick, G.D., Brown, J.H., Crowther, R.L., et al.: Binding of influenza virus hemagglutinin to analogs of its cell-surface receptor, sialic acid: analysis by proton nuclear magnetic resonance spectroscopy and X-ray crystallography. Biochemistry **31**, 9609–9621 (1992)
32. Bianco, A., Brufani, M., Ciabatti, R., Melchioni, C., Pasquali, V.: Neuraminic acid derivatives as anti-influenza drugs. Mol. Online **2**, 129–136 (1998). doi:10.1007/s007830050068

33. Brocca, P., Berthault, P., Sonnino, S.: Conformation of the oligosaccharide chain of GM1 ganglioside in a carbohydrate-enriched surface. Biophys. J. **74**, 309–318 (1998)
34. Sabesan, S., Bock, K., Lemieux, R.U.: The conformational properties of the gangliosides G_{M2} and G_{M1} based on ^{1}H- and ^{13}C-NMR studies. Can. J. Chem. **62**, 1034–1045 (1984)
35. Sharmila, D.J.S., Veluraja, K.: Conformations of higher gangliosides and their binding with cholera toxin-investigation by molecular modeling, molecular mechanics, and molecular dynamics. J. Biomol. Struct. Dyn. **23**, 641–656 (2006)
36. DeMarco, M.L., Woods, R.J.: Atomic-resolution conformational analysis of the GM3 ganglioside in a lipid bilayer and its implications for ganglioside-protein recognition at membrane surfaces. Glycobiol. **19**, 344–355 (2009)
37. Sharrow, S.D., Edmonds, K.A., Goodman, M.A., Novotny, M.V., Stone, M.J.: Thermodynamic consequences of disrupting a water-mediated hydrogen bond network in a protein: pheromone complex. Protein Sci. **14**, 249–256 (2005)
38. Patel, R.Y., Balaji, P.V.: Characterization of the conformational and orientational dynamics of ganglioside GM1 in a dipalmitoylphosphatidylcholine bilayer by molecular dynamics simulations. Biochim. Biophys. Acta (Biomembranes) **1768**, 1628–1640 (2007)